VOL. 14, NO. 4, FEBRUARY 2019 ISSN 1819-6608
ARPN Journal of Engineering and Applied Sciences

www.arpnjournals.com

SYNTHESIS AND CHARACTERIZATION OF ZINC TUNGSTATE OXIDES FILMS BY ADVANCED CONTROLLED CHEMICAL SPRAY PYROLYSIS DEPOSITION TECHNIQUE

Zena A. Salman, Alaa A. Abdul-Hamead and Farhad M. Othman
Materials Engineering Department, University of Technology, Baghdad, Iraq
E-Mail: zena_eng87@yahoo.com

ABSTRACT

For the first time zinc tungstate semiconductor oxides films ($ZnWO_4$) was successfully synthesized simply by advanced controlled chemical spray pyrolysis deposition technique, via employed double nozzle instead of single nozzle using tungstic acid and zinc chloride solutions at three different compositions and spray separately at same time on heated silicone (n-type) substrate at 600 °C, followed by annealing treatment for one hour at 500 °C. The crystal structure, microstructure and morphology properties of prepared films were studied by X-ray diffraction analysis (XRD), electron scanning electron microscopy (SEM) and atomic force microscopy (AFM) respectively. According to characterization techniques, a material of well-crystallized monoclinic phase $ZnWO_4$ films with rod-type 1D microstructures close to needle structure were obtained from using this advance technique, with thickness about 500 nm. Such these structures have been recognized as one of the most efficient microstructures especially in gas sensor applications due to their large specific surface area.

Keywords: $ZnWO_4$, semiconductor oxides, thin film, advance spray pyrolysis method, microstructure characterization.

1. INTRODUCTION

There is a proceeding requirement for particularly designed semiconductors that has prompted an enthusiasm in ternary oxides. Ternary oxides give more noteworthy adaptability to tune the chemical and physical characterization of the materials by changing their structure [1]. Pairing distinctive semiconductors permits the vectorial relocation of electrons starting with one semiconductor then onto the next, prompting an increasingly productive electron/gap partition and more noteworthy catalytic reactivity [2]. The control of semiconductor composition, Morphology, and microstructure are required for improving the characteristic of different oxides [3].

In the current years, tungsten compounds have been paid lots of attention because of their fantastic physical and chemical characterization. Tungsten compounds such as, tungsten oxides, carbides, nitrides, sulfides, bronzes, tungstate, tungsten metal has very wealthy chemistry materials, and they're all important commercial materials. They can be utilized in catalysis, electrical applications, photovoltaic cells, humidity and gaseous detecting and different chromogenic fields, scientific and dental applications [4].

Metal tungstate (MWO_4) were solidified with the wolframite kind of structure which can be depicted as composed of hexagonal close-packed oxygen atoms with specific octahedral locales filled by M^{2+} and W^{6+} cations in an arranged way. Combination having a place with this family was experienced as gas sensors or catalysts. The metal tungstate family mixes, for example $ZnWO_4$, $MnWO_4$, $FeWO_4$, $CoWO_4$, $NiWO_4$, $SnWO_4$ and $CuWO_4$ have been mostly researched [5]. Specifically zinc tungstate ($ZnWO_4$) possessing a high application potential in various fields, such as scintillator material, photoluminescence, electronic and optical properties, photovoltaic property, humidity sensor, hydrogen sensor, ether sensor, photo-catalyst and high-power lithium-ion batteries [6]. It was recognized as essential photo catalysts, optical fibers, gas detector and solid-state laser hosts [7]. In recent years, there has been growing interest in zinc tungstate ($ZnWO_4$) as a possible new material for sensor material for detection gases [8]. At ambient conditions, $ZnWO_4$ crystallize with wolframite structure that has monoclinic unit cell [9]. $ZnWO_4$, is a wide-gap semiconductor, with band gap energy close to 4 eV [10].

Numerous oxide blend can be custom fitted to accomplish wanted surface to volume proportions and morphologies as to achieve different gas detecting efficiency. The addition of a second component may cause a decline in the grain size, which likewise enhances gas sensor reaction properties [11]. Blending of metal oxides in a sensor layer has lately been investigated to enhance sensor efficiency and thermal stability. The blended oxides can possibly profit by the best detecting properties of their unmixed oxides. The electronic structures of the oxides are altered, bringing about change to both the mass and surface characterization [12]. Numerous researchers have investigated the possibilities of various morphologies of metal oxide semiconductor (MOS) one dimensional (1D)for example, wires, belts and needles micro and nano-structured materials as field-producers because of their low work capacities, high aspect proportions, high mechanical dependable qualities and conductivities, and wide applications in materials science, and especially in gas detecting applications [7]. It is important that the affectability of substance gas sensors is unequivocally influenced by the particular surface of detecting materials. A higher particular surface of a detecting material prompts higher sensor affectability. Subsequently, numerous systems have been received to build the particular surface

of detecting films with fine structured, taking advantage of the large specific surface of fine structured materials [13]. The properties of $ZnWO_4$were observed to be firmly linked with its morphology, crystallinity and particle size distribution subsequently relies upon its way of preparation [14]. $ZnWO_4$ particles have been synthesized by various routes such as polymerized complex method, microwave assisted technique, hydrothermal, ligand-assisted hydrothermal, template-free hydrothermal, solid-state reaction, polyol-mediated synthesis, solid-state metathetic approach, mechanochemical synthesis, sol-gel, calcining co-precipitated precursor and combustion method, electro-deposition and high direct voltage electro-spinning process [6]. In spray pyrolysis method has been carried out to board range of synthesis thin and thick layers. Even multi-layered dense and porous films and powders can be readily synthesis utilizing this adaptable method [15]. These layers were utilized in different equipment, for example, solar cells, sensors, and solid oxide fuel cells [13].The properties of precipitate layer relay on the conditions of fabrication [16].

Therefore, we report a technique that could success-fully prepare $ZnWO_4$ film by advanced controlled chemical spray pyrolysis deposition technique, the suggest process is easy, rapid, clean and actively efficient for preparation of microcrystalline materials with controlled size and shape and high density of surface area, which are suitable for technological applications such as gas sensor application.

2. MATERIALS AND EXPERIMENTAL WORKS

2.1 Materials used and preparation method

The zinc tungstate oxides films prepared by advance controlled chemical spray pyrolysis deposition technique using double nozzle by spray aqueous solutions of tungstic acid (H_2WO_4) and zinc chloride ($ZnCl_2$) separately at same time with molarity (0.1 M) at three different compositions are summarized in Table-1. The material mass was determined according to equation ($W=M_W*V_L*M/1000$), where M_w is molecular weight of material (gm/mol), M is material molarity (mol/L), V_L is volume of distilled water (ml) and W is material mass (gm) [17].

Table-1. Mixing percentages of salts.

Salts	Samples mix %			
	S	S1	S2	S3
H_2WO_4	100%	3	1	1
$ZnCl_2$	0	1	1	3

Silicon wafers were used to deposit films which was n-type, orientations <100> with resistivity of (0.65-0.95 Ω-cm), and (625µm) thickness. The silicon wafers cut to ($1cm^2$) dimensions and emersion in diluent (1:10) HF: H_2O for (10 min) to remove native oxides layer after that put in ultrasonic bath with ethanol Alcohol for 15 min then washed by distilled water and finally dried by air blowing and wiped with soft paper. Samples preparation shown in Figure-1.

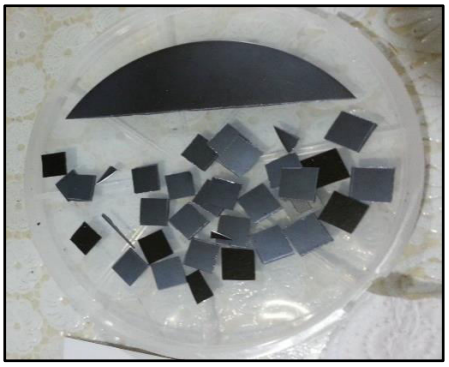

Figure-1. Silicon wafers preparation.

The whole spray system is homemade consists of the following: heater and thermocouple (k-type), double nozzle 1mm diameter with valve, electrical timer, air compressor, electrical gas valve and connectors as shown in Figure-2.

Figure-2. Spray system.

2.2 Thin film deposition procedure

First the salts were dissolved after knowing the molecular weights in a certain volume of distilled water 20ml and placed on the magnetic stirrer for 20 min until the solution get homogeneous and to ensure that the material is completely dissolved. The solutions were then put into the bottle of the two nozzles and then the substrate was placed in the middle of the surface of the heater and left to reaches the required temperature which was

measured using a thermocouple, the substrates were fixed on heater by Maxi aluminum adhesive conductive tape and heated to reach the required temperature, the optimum substrate temperature was found to be 600 °C, because the reaction is not completed in the less temperature. After all these steps were done, then solution was sprayed and make sure the droplets of solution is falling in regular manner on the substrate surface. The spraying time of the solution was controlled by electrical timer and electrical gas valve, the deposition time was (3sec) each (1-2 min) thus the substrates no loss the thermal stability. After finishing the deposition, the substrate left to cool to the ambient temperature to avoid any thermal stresses which may cause to broke or get distortions in the layer.

The other parameters like pressure spray rate and spray distance technique are summarized in Table-2. After the deposition, the prepared samples were annealed for one hour at 500 ˚C and let the samples cooling inside furnace. This step is done for improving the quality and crystallinity of the films according to author [18].

Table-2. Process parameters.

Process conditions	Value
Pressure	7 bar
Air flow rate	8 cm^3/sec
Spray distance	25 ±1 cm
Spray solution size	20 ml
Feeding rate	2.5 ml/min
Spatter number	20
Period between Spatter	1-2 min

3. MATERIALS CHARACTERIZATION

The crystal structure and phase identification of the films after annealing were characterized by X-ray diffraction (XRD) inspection with radiation CuKα (λ=1.5406 °A),The X-Ray diffraction investigations were conducted by using SHIMADZU XRD-7000 MAXima, the target is Cu beam with an angle from (10 to 60) with 40 KV & 30 mA.

The microstructures of the samples were investigated by scanning electron microscopy (SEM) is one of the most commonly used surface analysis techniques in which a wide range of scales and feature can be observed. Scanning electron microscope attached with energy dispersive X-ray (EDX) examination was used to reveal the microstructure and chemical composition of samples

The surface roughness test was performed by using the surface roughness tester (AFM) device supplied with a sensor which moves linearly along the measured length.

The thickness of prepared samples was determine by utilizing the optical interferometer method that is depend on interference of the light beam reflection from sample surface and substrate bottom. Laser type He-Ne (632 nm) is used and the thickness can be obtained by using the formula below [19], and was calculated to be approximately 500 nm.

$$T = \frac{\Delta X}{X} * \frac{\lambda}{2} \quad (1)$$

Where:

T = Thickness of the film in (nm).
X = Width of fringe (cm).
ΔX = Distance between two fringes (cm).
λ = Length of wave of laser light (nm).

4. RESULTS AND DISCUSSIONS

4.1 Crystal structure characteristics

The X-ray diffraction pattern was used to identify the phase present and their crystallite size is displayed between 10 and 60 2θ, which is the area in which the most intense peaks of tungstate oxides are observed. Figure-3 shows the X-ray spectra of pure tungsten oxide film WO_3 deposited onto silicone substrate at 300 °C. It is found that film is crystalline and corresponding with monoclinic crystal structure, the three predominant peaks correspond to the direction (002), (020) and (200). The diffraction peaks are agreed with data given in card (JCPDS No. 43-1035) data, as already reported by [20-22]. The XRD pattern shows broad peaks with small crystallinity due to small quantity of spray solution, recently researchers found that there is a relation between the quantity of solution and the thickness of layer deposited, by increasing the amount of solution the thickness of the layer increases, and the peaks intensity increases also due to increasing thickness of prepared layered [23]. Other researchers found that the substrate temperature and annealing temperature affected the phase of the WO_3 films prepared by spray pyrolysis, they reported that the as-deposited film below 350 °C exhibits either amorphous or consisted of very small crystallites, and at 400 °C exhibits crystalline structure [24] and [25]. No characteristic peaks of other compounds were observed. Table-3. Show results data of XRD sample (S). The average crystallite size of WO_3 sample is found in the range 2.4-3.7 nm was calculated by the Scherrer equation ($D=k\lambda/\beta\cos\theta$) [26], where:

D = Average crystallite size.
K = Scherrer constant.
λ = X-ray radiation wavelength.
β= Peak width at half height.
θ = Peak position corresponds.

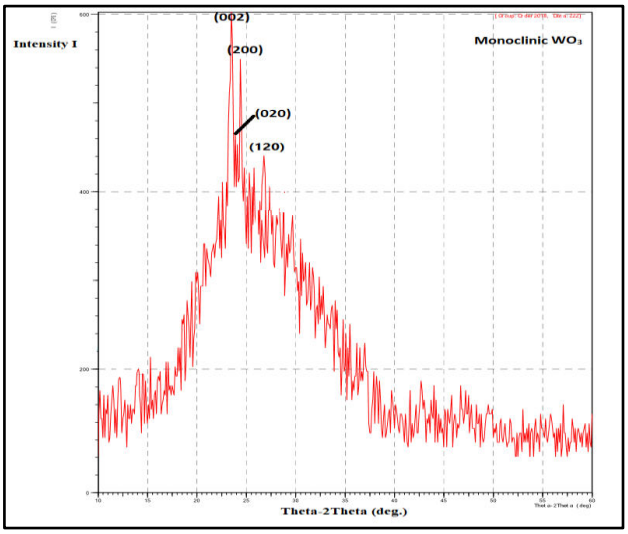

Figure-3. Shows the x-ray spectra of pure tungsten oxide film (S).

Table-3. Results data of XRD sample (S).

WO_3		
2θ (deg.)	(hkl)	**Intensity (c/s)**
23.12	002	100
23.59	020	97
24.39	200	99
	120	19

The Figures (4-6) show the XRD patterns result for (S1, S2 and S3) samples respectively. All of XRD spectrums could be indicated to highly crystallized monoclinic zinc tungsten oxides $ZnWO_4$ structure oriented (111) at intensity100%, that is match with JCPDS-PDF card file No. (15-0774), these findings confirm the formation of $ZnWO_4$ corroborating to the results from XRD analysis. An investigation of these data demonstrate that the relating values are predictable with results detailed by other authors [2] and [27]. The sharp diffraction features suggest the crystalline nature of all the samples. An increase in diffraction intensity indicates an increase in the crystallinity, which can be attributed to increasing substrate temperature and the annealing of the samples.

In Figure-4 show XRD pattern of sample (S1), the main peaks were indexed corresponding to a orthorhombic structure ofWO_3 which is match with the JCPDS-PDF card file No(20-1324), oriented at (001), (200), (021), (201), (220) and (400), its observed due to high content of tungsten salt and increasing of deposition temperature than sample (S) in Figure-3, while other peaks were indexed to monoclinic $ZnWO_4$ structure oriented at (011), (110), (111), (200) and (022). The sharp peaks of both phases that indicated the substrate temperature is suitable to obtain highly crystallized monoclinic $ZnWO_4$. The XRD patterns of the composites corresponds $ZnWO_4$–WO_3 only implying that there are no impurity peaks. Table-4. Show results data of XRD sample (S1).

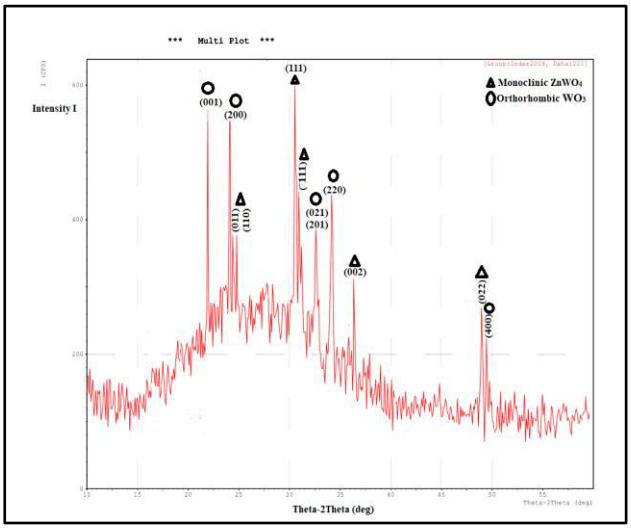

Figure-4. Shows the x-ray spectra of sample (S1).

Table-4. Results data of XRD sample (S1).

Compounds	**2θ** (deg.)	(hkl)	**Intensity** (c/s)
$ZnWO_4$	23.85	011	40
	54.58	110	35
	30.50	111	100
	30.70	$\bar{1}11$	90
	36.45	002	35
	48.75	022	14
WO_3	23.09	001	100
	24.08	200	95
	33.35	021	35
	33.64	201	25
	34.03	220	50
	49.33	400	20

In Figure-5 show XRD pattern of sample (S2), all diffraction peaks can be readily indexed to a pure monoclinic phase of $ZnWO_4$ (JCPDS card No. 15-0774), No additional peak of other phases has been found, which indicates that the synthesized sample is single-phase, due to equivalent ratios of solutions.Table-5. Show results data of XRD sample (S2). In Figure-6 show XRD pattern of sample (S3), the XRD spectra was indicated to combination of $ZnWO_4$as the major and ZnO as minor phases. The major peaks were indexed corresponding to monoclinic phase of $ZnWO_4$ (JCPDS card No. 15-0774). It observed broad peaks of pure $ZnWO_4$in beginning and sharp in ending that indicating to exist more than one peak at one position (2θ). The minor peaks are indexed on basis of the crystallographic data of the known structure hexagonal ZnO all the diffraction lines agree with reported values and match with the JCPDS data (036-1451) due to increasing zinc salts in this sample. No characteristic

peaks of other compounds such as WO_3were observed. Table-6. shows results data of XRD sample (S3).

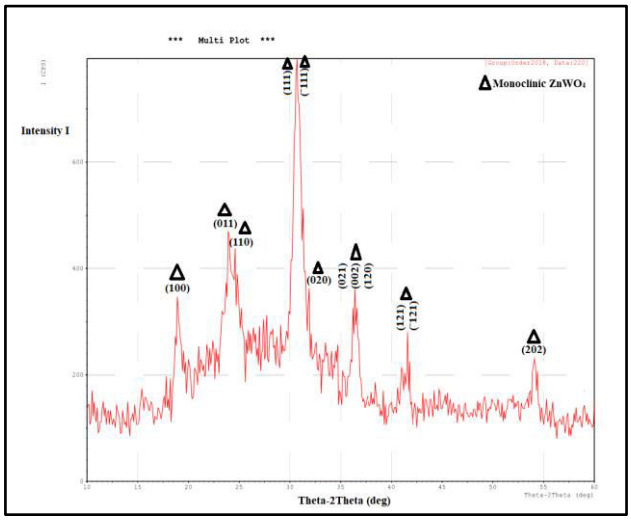

Figure-5. Shows the x-ray spectra of sample (S2).

Table-5. Results data of XRD sample (S2).

Compounds	2θ (deg.)	(hkl)	Intensity (c/s)
$ZnWO_4$	23.85	011	40
	54.58	110	35
	30.50	111	100
	30.70	-111	90
	36.45	002	35
	48.75	022	14
WO_3	23.09	001	100
	24.08	200	95
	33.35	021	35
	33.64	201	25
	34.03	220	50
	49.33	400	20

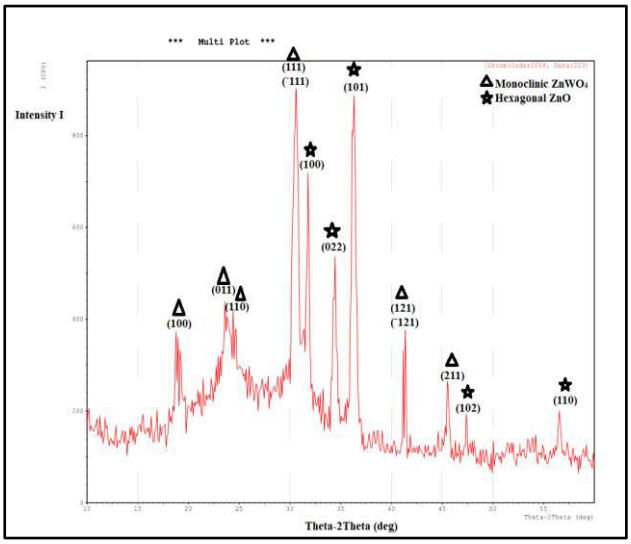

Figure-6. Shows the x-ray spectra of sample (S3).

Table-6. Results data of XRD sample (S3).

Compounds	2θ (deg.)	(hkl)	Intensity (c/s)
$ZnWO_4$	23.85	011	40
	54.58	110	35
	30.50	111	100
	30.70	-111	90
	36.45	002	35
	48.75	022	14
ZnO	23.09	001	100
	24.08	200	95
	33.35	021	35
	33.64	201	25
	34.03	220	50
	49.33	400	20

The mean crystallite size of $ZnWO_4$ was calculated from X-ray line broadening analysis using the Scherrer equation above. The mean crystallite size of $ZnWO_4$ was found to be approximately 16.51, 19.37 and 24.62 nm of S1, S2, and S3 samples respectively, and found to be 17.05nm of WO_3 in sample S1 and 18.3 nm ZnO of samples S3.No characteristic peak of impurity was detected on XRD patterns meaning that the materials exhibits a high degree of purity.

4.2 Microstructural characteristics (SEM&EDX)

The morphology of the prepared samples was studied by SEM, Figures (7-14) show a microstructure photographs with EDX charts of annealed samples. It is revealed that the prepared precipitate is well-crystalline formed under the current synthesis condition, which agrees well with the results of XRD. In Figure-7 show fibrousWO_3microstructurelike network, and have a

uniform, filamentous (like chain) surface morphology and variable length filaments distribute all over the surface. It could be observed that intensity of the filamentous structure is low due to small quantity of spray solution, and that agree with XRD result [23]. The chemical composition EDX result in Figure-8 of sample (S) after heat treatment index to pure WO_3 film oxide in close agreement with the nominal compositions and did not show any impurity elements.

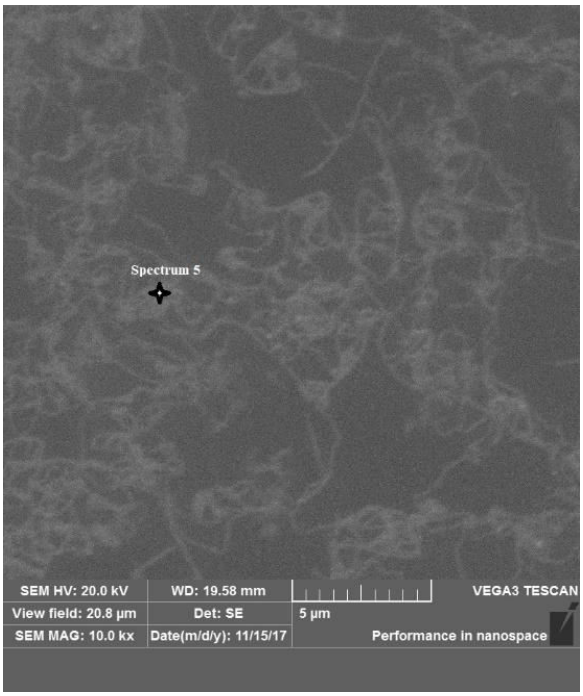

Figure-7. SEM micrograph image of the sample (S).

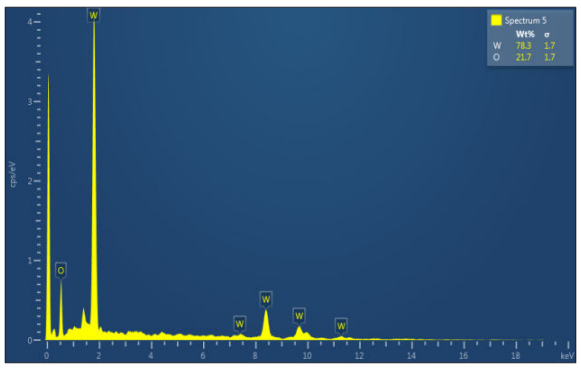

Figure-8. EDX charts of the sample (S).

In figure-9 shows a representative SEM image of as-annealed sample (S1) thin film.There is a low quantity of rod-type 1D microstructures close to needle structure with different length, is found in the range 3-4µm, and 0.5 µm width. This is consistent with what previous researchers have found [27] and [7]. The SEM image also reveals presence smaller aggregated of WO_3 due to high tungsten precursor concentration in this sample. The chemical composition of sample (S2) thin film was validated by EDX analysis. Figure-10 shows close agreement with the nominal mixed compositions and did not show any impurity elements. The EDX spectrum showed the presence of only W, Zn and Oindicating a successful preparation procedure, and that agree with SEM and XRD results.

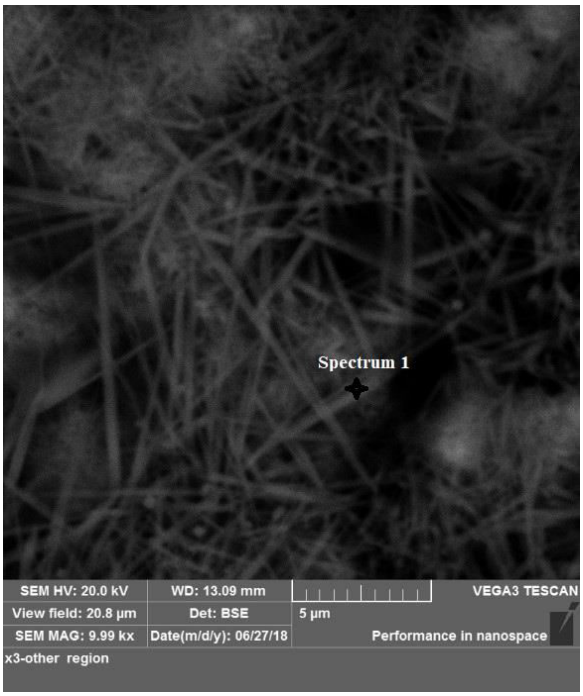

Figure-9. SEM micrograph image for the sample (S1).

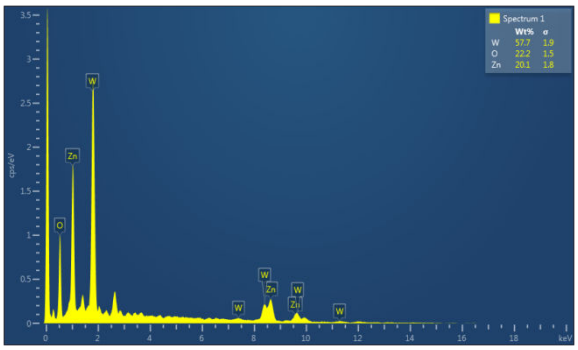

Figure-10. EDX charts of the sample (S1).

In Figure-11 shows a representative SEM image of as-annealed sample (S2) thin film. The microstructure indicated to only$ZnWO_4$ phase, with high density of aggregated uniform rod-type 1D microstructure comparing with S1 sample, due to increase content of Zn salt. This sample were composed of the whole micro-rods of $ZnWO_4$with the average length and diameter of 4µm and1µm respectively. This microstructures possess high surface area, thus by using this advanced technique The chemical composition EDX result for the composition of sample (S2) after heat treatment in figure-12 index to pure $ZnWO_4$ film oxide. Note only Zn, W and O were detected, in close agreement with the nominal compositions and did not show any impurity elements, and that agree with XRD result.

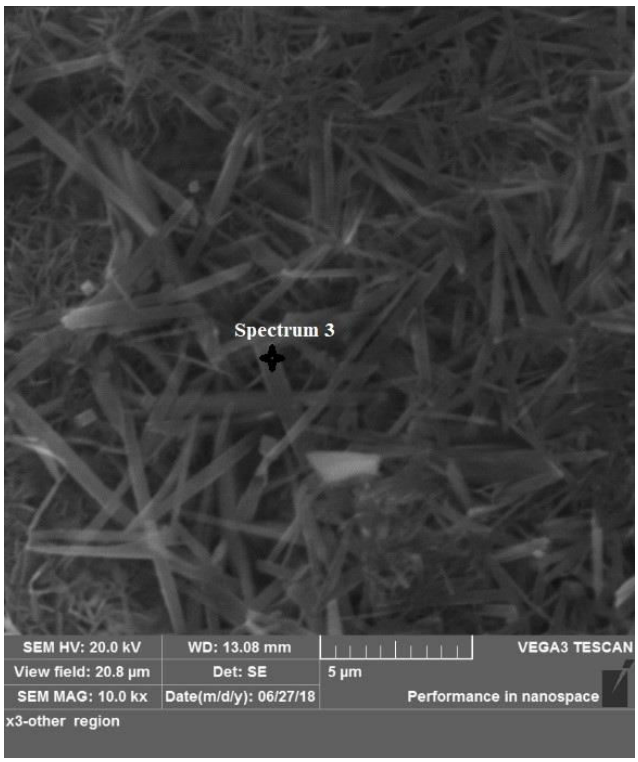

Figure-11. SEM micrograph image for the sample (S2).

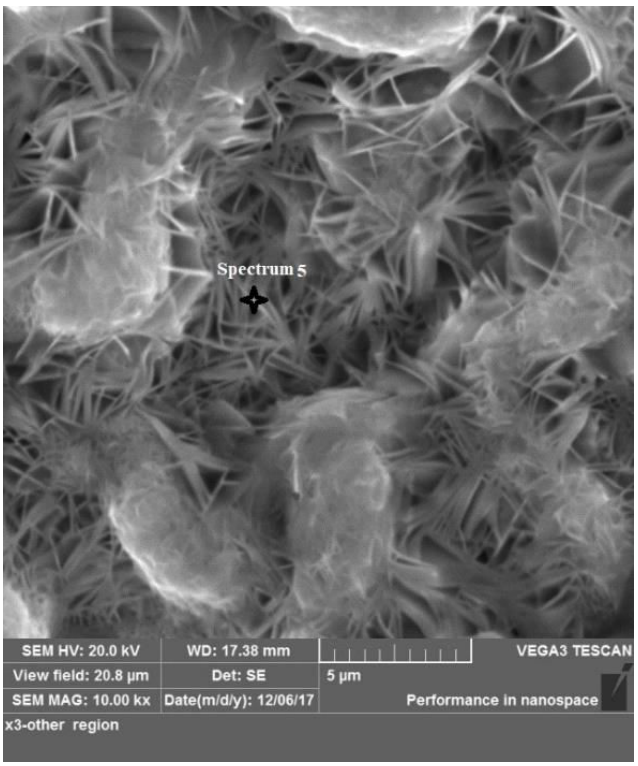

Figure-13. SEM micrograph image for the sample (S3).

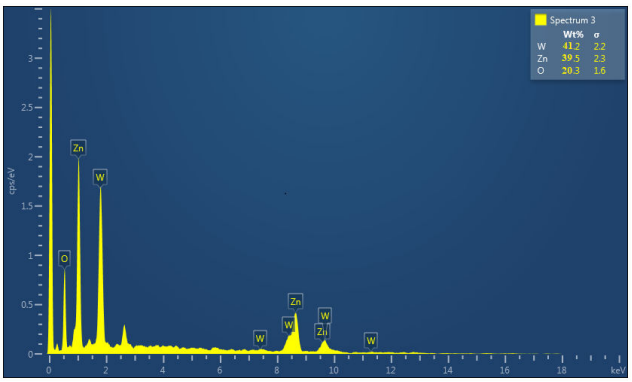

Figure-12. EDX charts of the sample (S2).

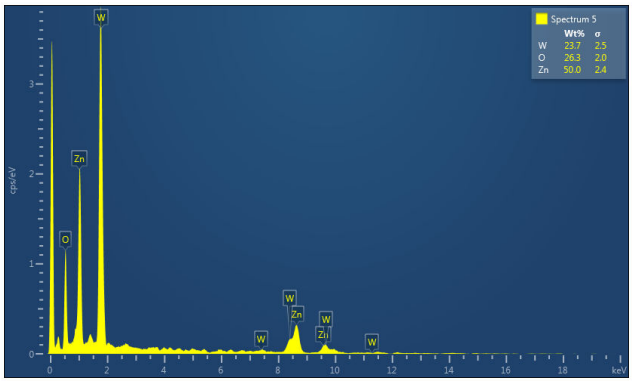

Figure-14. EDX charts of the sample (S3).

In Figure-13 shows a representative SEM image of as-annealed sample (S3) thin film. It found by increasing Zn salt content, ZnO oxide appear as major phase with $ZnWO_4$ oxide as minor phase. The high-magnification SEM images show that microstructure indicated to of rod-type 1D $ZnWO_4$ oxideless dense comparing to sample (S2). The average length of $ZnWO_4$micro-rode became fine and shorter close to be 2 µm and with width approximately 0.5µm. The chemical composition EDX result for the composition of sample (S3) after heat treatment in figure-12 index to composites correspond $ZnWO_4$–ZnO. Note also that only Zn, W and O were detected, in close agreement with the nominal compositions and did not show any impurity elements, and that agree with XRD result

4.3 Morphological characteristics (AFM)

The morphology of surface of samples was analyzed by using atomic force microscope, and also used to determine average diameter of particles of films and its distribution. This surface characteristic is important for applications such as gas sensors and catalysts. Figures (15-18) shows the typical two and three dimensional AFM image with granularity accumulation distribution chart of samples. AFM images show that the all films are well faceted crystallites, uniformly packed and were small grain; this means that the prepared films are well deposited.Table-7 show the variation of root mean square, average roughness and average diameter of annealed samples.

It's observed that the average roughness and root mean square of pure WO_3 film sample (S) S1 found to be1.19 nm and 1.45 nm respectively, and it is increased with decreasing the tungsten salt, that mean by addition of

zinc salt the average roughness and root mean square increase, and the highest value at sample (S2) 6.67 nm and 7.7 nm respectively, when the proportion of solutions is equal, and became less in sample (S3) when the proportion of zinc salt is reduced.

Granularity accumulation distribution charts of all sample show that the particles on the surface of the film have different diameter values with narrow range and displays a statistical distribution for the particle diameter over the surface and it acceptable value for gas sensor application as reported by researcher [28].

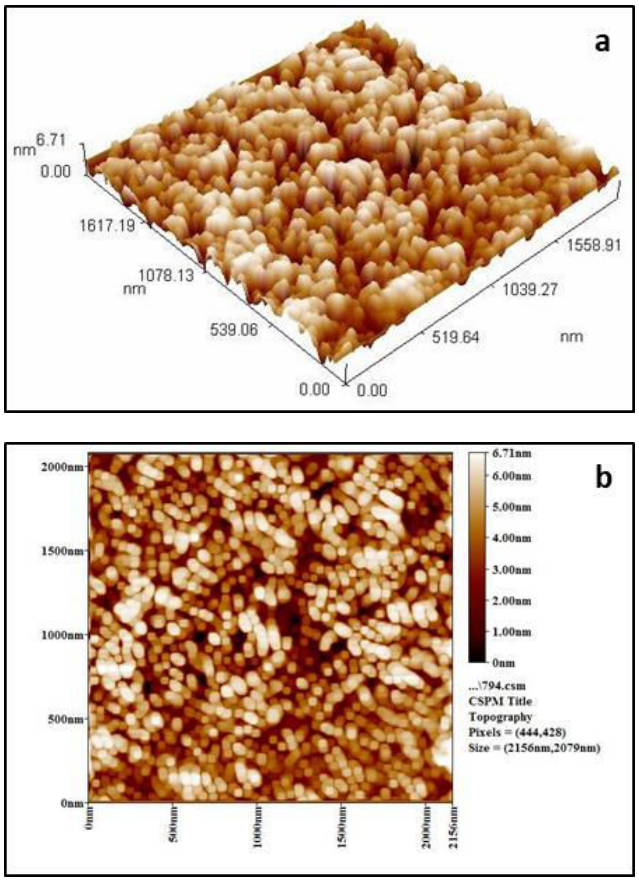

Figure-15. AFM image (a) 3D, (b) 2D and (c) Granularity accumulation distribution chart of the sample (S).

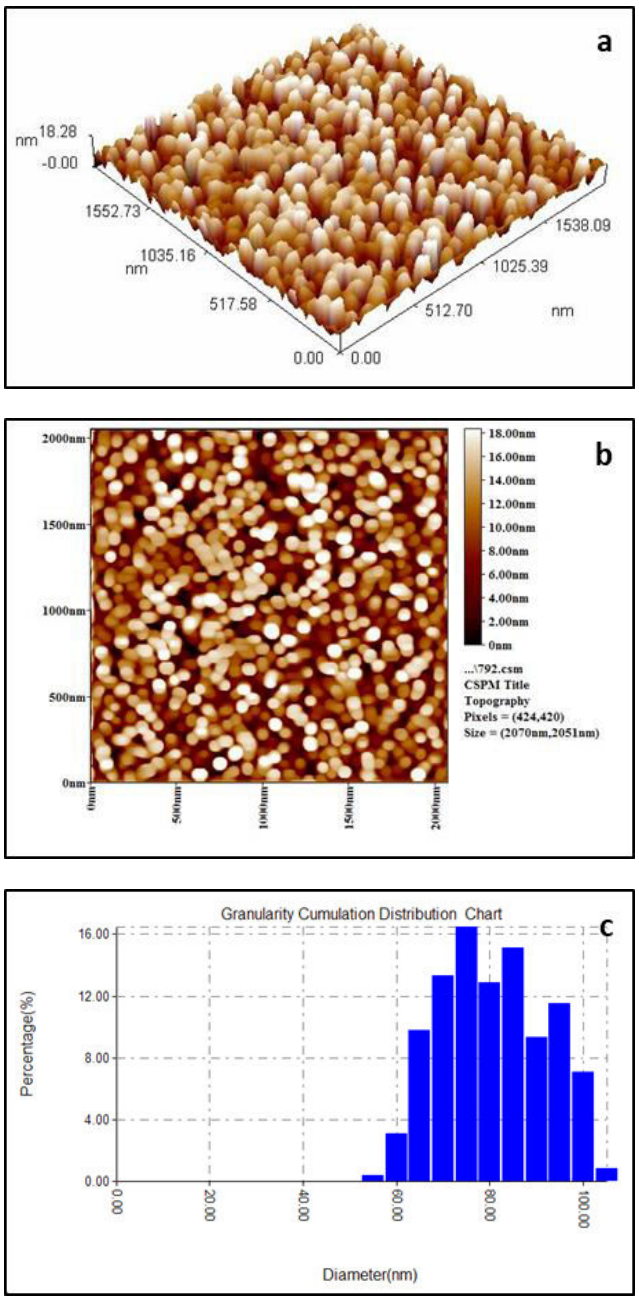

Figure-16. AFM image (a) 3D, (b) 2D and (c) Granularity accumulation distribution chart of sample (S1).

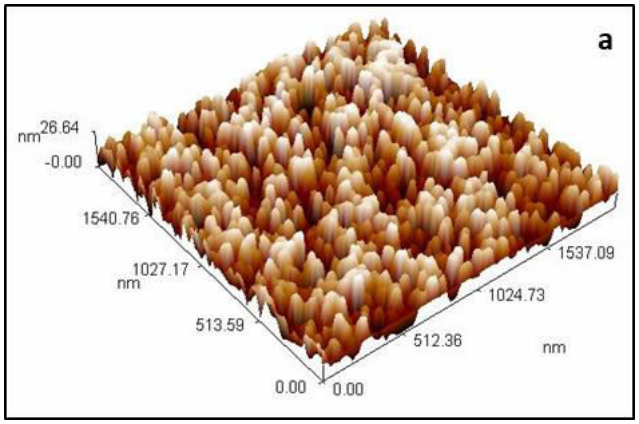

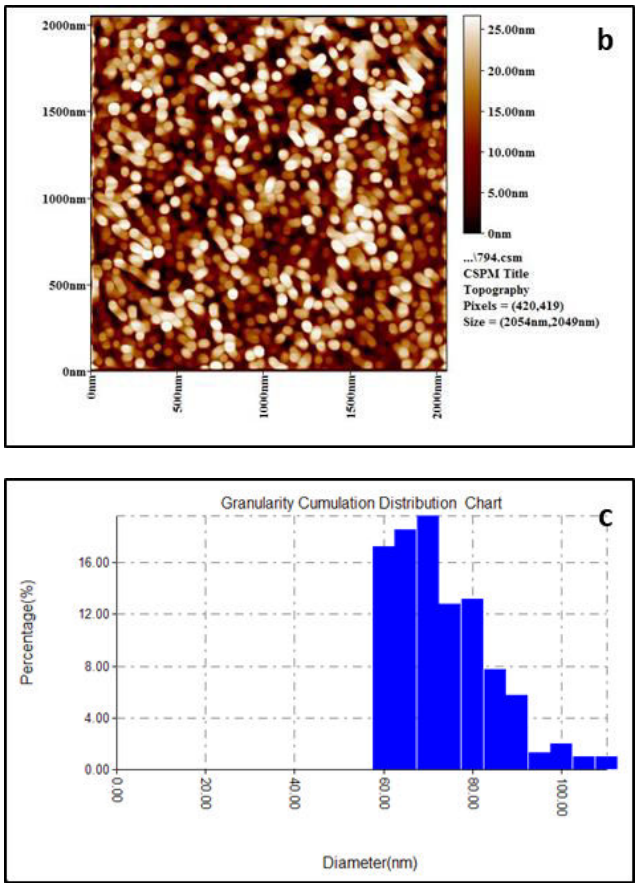

Figure-17. AFM image (a) 3D, (b) 2D and (c) Granularity accumulation distribution chart of sample (S2).

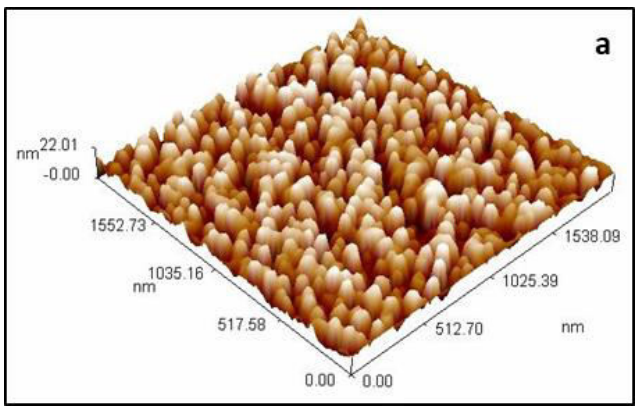

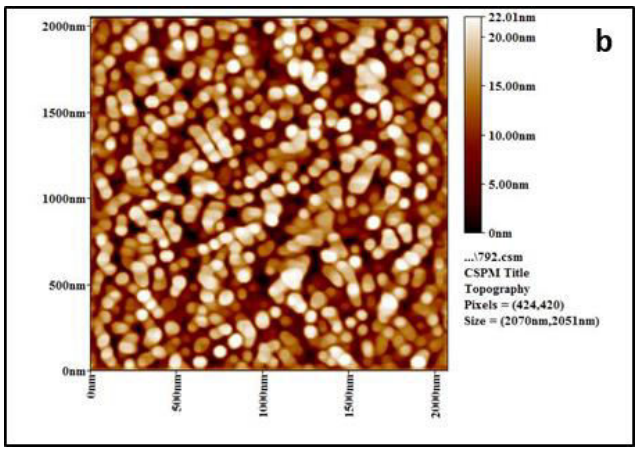

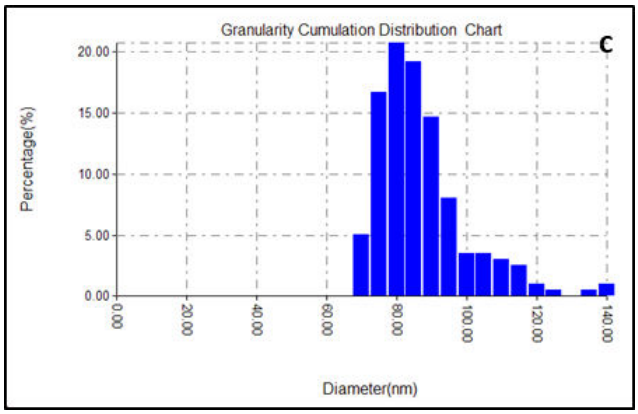

Figure-18. AFM image (a) 3D, (b) 2D and (c) Granularity accumulation distribution chart of sample (S3).

Table-7. Variation of root mean square, average roughness and average diameter of samples.

Samples	Roughness average(nm)	Root mean square(nm)	Diameter average(nm)
S	1.19	1.45	54.89
S1	3.96	4.67	78.19
S2	6.67	7.7	70.75
S3	4.62	5.51	84.79

5. CONCLUSIONS

a) It could conclude that spray pyrolysis technique using double nozzles and the substrate temperature are suitable to obtain crystallized monoclinic zinc tungsten film $ZnWO_4$.

b) Spray pyrolysis method by employed double nozzles exhibits rod-type 1D microstructures close to needle structure to $ZnWO_4$microstructure and this type is most efficient microstructures especially in gas sensor applications due to large specific surface area.

c) From XRD and SEM results, it can be concluded that the content of zinc salt influenced the phase and morphology of $ZnWO_4$film synthesized advanced spray pyrolysis technique. Increase the zinc salt content has altered the shape topography and microstructure of the prepared samples; this is

reflected in the changing ratio of the phases formed with various percentages of zinc salt.

REFERENCES

[1] Tharsika T., Haseeb A.S.M.A., Akbar S.A., Sabri M.F.M. & Wong Y.H. 2015. Gas sensing properties of zinc stannate (Zn_2SnO_4) nanowires prepared by carbon assisted thermal evaporation process. Journal of Alloys and Compounds. 618(1): 455-462.

[2] Hamrouni A., Moussa N., Paolab A. D., Parrino F., Houasa A. & Palmisano L. 2014. Characterization and photoactivity of coupled ZnO-$ZnWO_4$catalysts prepared by a sol-gel method. Applied Catalysis B: Environmental. 154-155(1): 379-385.

[3] Ghimbeu C. M. 2007. Preparation and Characterization of metal oxide semiconductor thin films for the detection of atmospheric pollutant gases. Ph.D Thesis, University Paul Verlaine of Metz.

[4] Kovacs T. N., Pokol G., Gaber F., Nagy D., Igricz T., Lukacs I. E., Fogarassy Z., Balazsi K., Szilagyi I. M.2017. Preparation of iron tungstate ($FeWO_4$) nanosheets byhydrothermal method. Materials Research Bulletin. 95(1): 563-569.

[5] Dan M., Cheng M., Gao1 H., Zheng H. & Chuanqi Feng. 2014. Synthesis and Electrochemical Properties of $SnWO_4$. Journal of Nanoscience and Nanotechnology. 14(1): 2395-2399.

[6] Severo E. d. C., Abaide E. R., Anchieta C. G., Foletto V. S., Weber C. T., Garlet T. B., Collazzo G. C. , Mazutti M. A., Gündel A. , Kuhn R. C. & Foletto E. L. 2016. Preparation of Zinc Tungstate ($ZnWO_4$) Particles by Solvo-hydrothermal Technique and their Application as Support for Inulinase Immobilization. Materials Research. 19(4): 781-785.

[7] Siriwong P., Thongtem T., Phuruangrat A. & Thongtem, S. 2011. Hydrothermal synthesis, characterization, and optical properties of wolframite $ZnWO_4$ nanorods. Cryst Eng Comm. 13(5): 1564-1569.

[8] Phani A.R., Passacantando M., Lozzi L. & Santucci,S. 2000. Structural characterization of bulk $ZnWO_4$ prepared by solid state method. Journal of materials science. 35(19): 4879-4883.

[9] De Oliveira A. L. M., Ferreira J. M., Márcia R.S.S., De Souza S. C., Vieira F. T. G., Longo E., Souza A. G. & Santos I. M.G. 2009. Influence of the thermal treatment in the crystallization of $NiWO_4$ and $ZnWO_4$. Journal of thermal analysis and calorimetry. 97(1): 167-172.

[10] Minh N. V. & Hung N. M. 2011. A Study of the Optical Properties in $ZnWO_4$ Nanorods Synthesized by Hydrothermal Method. Materials Sciences and Application. 2(1): 988-992.

[11] Galatsis K., Li Y.X., Wlodarski W., Comini E., Sberveglieri G., Cantalini C., Santucci S. & Passacantando M. 2002. Comparison of single and binary oxide MoO_3, TiO_2 and WO_3 sol-gel gas sensors. Sensors and Actuators B: Chemical. 83(1-3): 276-280.

[12] Ilegbusi O.J., Khatami S.N. & Trakhtenberg L.I. 2017. Spray Pyrolysis deposition of single and mixed oxide thin films. Materials Sciences and Applications. 8(02): 153-169.

[13] X. Peng. 2012. Nanowires - Recent Advances. InTech Publisher. Croatia. Chapter1: 3-23.

[14] Nasrabadi R. M., Pourmortazavi S.M., Rezvani Z., Adib K. & Ganjali M.R. 2015. Facile synthesis optimization and structure characterization of zinc tungstate nanoparticles. Materials and Manufacturing Processes. 30(1): 34-40.

[15] Perednis D. & Gauckler L.J. 2005. Thin film deposition using spray pyrolysis. Journal of electroceramics. 14(2): 103-111.

[16] Perednis D. 2003. Thin film deposition by spray pyrolysis and the application in solid oxide fuel cells. Ph.D. Thesis. Swiss Federal Institute of Technology Zurich. Lithuania.

[17] Baysinger G. & Berger L. I. 2003. CRC Handbook of Chemistry and Physics. 96th Edition. CRC publication. National Institute of Standards and Technology.

[18] Long N.V., Teranishi T., Yang Y., Thi C.M., Cao Y. & Nogami M. 2015. Iron oxide nanoparticles for next generation gas sensors. International Journal of Metallurgical & Materials Engineering. 1: 1-18.

[19] Hernandez M., Juarez A. & Hernandez R. 1999. Interferometric thickness determination of thin metallic films. Superficies y vacío. 9(1): 283-285.

[20] Sivakumar R., Raj A.M.E., Subramanian B., Jayachandran M., Trivedi D.C. & Sanjeeviraja C.

2004. Preparation and characterization of spray deposited n-type WO_3 thin films for electrochromic devices. Materials Research Bulletin. 39(10): 1479-1489.

[21] Grace P.S., Devadasan J.J., Thangam G.J., Sanjeeviraja C. 2014. Synthesis and Characterization of Tungsten Trioxide (WO_3) Thin Films by Advanced Microprocessor Controlled Spray Pyrolysis Method. International Journal of ChemTech Research. 6(13): 5382-5386.

[22] Choi H.G., Jung Y.H. & Kim D.K. 2005. Solvothermal synthesis of tungsten oxide nanorod/nanowire/nanosheet. Journal of the American Ceramic Society. 88(6): 1684-1686.

[23] Karadeniz S. M. & Ekinci A. E. 2014. XRD and SEM Results of WO_3 Thin Films Deposited on Quartz Glasses. International Journal of Applied Science and Technology. 4(5): 136-139.

[24] Hao J., Studenikin S.A. & Cocivera M. 2001. Transient photoconductivity properties of tungsten oxide thin films prepared by spray pyrolysis. Journal of Applied Physics. 90(10): 5064-5069.

[25] Kim C.Y., Cho S.G., Park S. & Choi D.K. 2009. Tungsten oxide film synthesis by spray pyrolysis of peroxotungstic acid and its electrochromic characterization. Journal of Ceramic Processing Research. 10(6): 851-854.

[26] Eranjaneya H. & Chandrappa G.T. 2016. Solution combustion synthesis of nano $ZnWO_4$ photocatalyst. Transactions of the Indian Ceramic Society. 75(2): 133-137.

[27] Dai R.C., Wang Z.P., Zhang Z.M. & Ding Z.J. 2014. Characterizations, structure and optical properties of $ZnWO_4$: Eu nanorods under high temperature. Surface and Interface Analysis. 46(12-13): 1151-1155.

[28] Hantoosh A. K. 2015. Fabrication and Characterization of CdS/PbS Solar Cell by Chemical Spray Pyrolysis. MSc. Applied Sciences. University of Technology. Baghdad. Iraq.